

Dynamical Variational Approach to Bose Polarons at Finite Temperatures

David Dzsotjan,^{1,2} Richard Schmidt^{3,4} and Michael Fleischhauer¹

¹Department of Physics and Research Center OPTIMAS, University of Kaiserslautern, 67663 Kaiserslautern, Germany

²Wigner Research Center, Konkoly-Thege ut 29-33, 1121 Budapest, Hungary

³Max-Planck-Institute of Quantum Optics, Hans-Kopfermann-Strasse. 1, 85748 Garching, Germany

⁴Munich Center for Quantum Science and Technology (MCQST), Schellingstr. 4, 80799 München, Germany



(Received 25 October 2019; accepted 13 May 2020; published 2 June 2020)

We discuss the interaction of a mobile quantum impurity with a Bose-Einstein condensate of atoms at finite temperature. To describe the resulting Bose polaron formation we develop a dynamical variational approach applicable to an initial thermal gas of Bogoliubov phonons. We study the polaron formation after switching on the interaction, e.g., by a radio-frequency (rf) pulse from a noninteracting to an interacting state. To treat also the strongly interacting regime, interaction terms beyond the Fröhlich model are taken into account. We calculate the real-time impurity Green's function and discuss its temperature dependence. Furthermore we determine the rf absorption spectrum and find good agreement with recent experimental observations. We predict temperature-induced shifts and a substantial broadening of spectral lines. The analysis of the real-time Green's function reveals a crossover to a linear temperature dependence of the thermal decay rate of Bose polarons as unitary interactions are approached.

DOI: 10.1103/PhysRevLett.124.223401

Introduction.—The interaction of a mobile impurity with a surrounding quantum bath is one of the paradigmatic models of many-body physics. The polaron introduced by Landau, Pekar, and Fröhlich [1,2] to describe the motion of an electron in a lattice of ions, is formed by the dressing with lattice phonons and is a prime example of quasiparticle formation in condensed matter. More recently, neutral atoms immersed in quantum degenerate gases of bosonic or fermionic atoms have attracted much attention since they are experimentally accessible platforms allowing to study polaron physics with high precision and in novel regimes. Employing Feshbach resonances [3] it is possible to tune the impurity-bath interaction from weak to strong coupling and Rydberg states can be used to study impurities with nonlocal interactions [4–6].

The problem of a Fermi polaron, i.e., an impurity interacting with a degenerate Fermi gas has been studied in a number of experiments in recent years [7–14]. This and related theoretical work [15–35] have led to a rather good understanding of this problem. In contrast, the description of impurities in a Bose-Einstein condensate (BEC), leading to the so-called Bose polaron is more involved [36]. The challenge for theory is here directly related to the relatively large compressibility of the system, which allows for a much larger number of excitations that can be generated by the impurity. Also the experimental observation presented a major challenge due to three-body losses, and has only recently been achieved in experiments at JILA [37], Aarhus [38], and MIT [39]. Tuning through a Feshbach resonance all regimes from weak to strong coupling were studied. While being in good general agreement with theoretical

predictions, the Aarhus data showed deviations for strong repulsive interactions, see Fig. 1, which were attributed to a nonzero temperature. Following up on that, a recent extended T -matrix analysis predicted rather dramatic

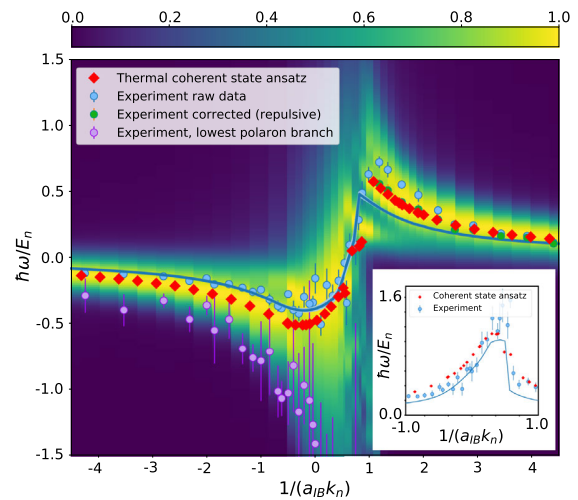


FIG. 1. Density averaged polaron absorption spectra $\bar{A}(\omega)$ from a noninteracting state of the impurity into an interacting state as a function of dimensionless impurity-boson scattering length $k_n a_{IB}$. $k_n = (6\pi^2 n)^{1/3}$ with n being the trapped-averaged density of the Bose gas (see Ref. [38]), and $E_n = k_n^2 / (2m_{\text{red}})$. Red dots show the mean peak values and HWHM width (inset) of the absorption spectrum predicted by the thermal coherent state variational ansatz (color code) at $T = 160$ nK compared with experimental results (blue and green symbols) from Refs. [38] and [42]. Full lines show the $T = 0$ theoretical predictions in Ref. [38].

temperature effects [40], most notably the appearance of new temperature-induced quasiparticle peaks [41], which would have profound consequences for the quasiparticle interpretation of the Bose polaron and its properties. These recent developments highlight the need of new theoretical approaches that take into account temperature as well as the creation of a large number of excitations in polaron formation. Indeed, while there exists by now a broad set of theoretical techniques to study Bose polarons at $T = 0$, extensions to $T > 0$ are not straightforward, so that, apart from first diagrammatic and functional determinant approaches [5,40,41], theoretical progress remains highly limited so far.

We here discuss the Bose polaron at nonzero temperature developing a dynamic variational approach for an initial state of Bogoliubov phonons at finite T , which for $T = 0$ simplifies to that of Ref. [43]. The method is a non-equilibrium one and thus gives direct access to the dynamics of polaron formation after an excitation from a noninteracting state by a rf pulse. One of the key results is depicted in Fig. 1, where we show the calculated, trap averaged absorption spectrum $\bar{A}(\omega)$ (color coding) for the Aarhus experiment. For $1/k_n a_{\text{IB}} > 0$ a notable difference between the peak positions of $T = 0$ calculations (full line) from the experimental values (blue circles: raw data [38] and green circles: corrected data [42]) was observed. In contrast, the results from our approach (red points) show good agreement. While the raw data exhibit a small deviation from our values on the attractive side [we define the mean peak response as $\bar{\omega} = \int d\omega \omega \bar{A}(\omega)$], the onset of the polaron branch (purple circles, [42]) matches well the onset of the theoretical absorption spectra. Strictly speaking, a sharp lower bound for the polaron energies (quantum Monte Carlo result in Ref. [42]) makes only sense at $T = 0$: for finite T the spectrum continues and goes smoothly to 0 shortly below this value. Moreover, the calculated width of the absorption peaks (inset) agrees well with the experiment. Finally, while our approach predicts temperature-induced shifts, thermal quasiparticle broadening, and a temperature-dependent quasiparticle weight, in contrast to Ref. [41] we do not find evidence for a significant transfer of spectral weight to new quasiparticle peaks, i.e., we do not see a transition from a single peak to two well-separated peaks as T becomes nonzero.

Model.—We here consider the interaction of a single impurity of mass M with a homogeneous Bose gas in d dimensions in a box of size L^d with periodic boundary conditions. Position and momentum operators of the impurity are \hat{r} and \hat{p} . We treat the BEC of condensate density n_0 in Bogoliubov approximation, i.e., in terms of noninteracting plane-wave excitations (phonons) of momentum \mathbf{k} , described by annihilation and creation operators $\hat{a}_{\mathbf{k}}^{(\dagger)}$. The condensate is characterized by the healing length $\xi = 1/\sqrt{2g_{\text{BB}}n_0m}$, where m is the mass of the BEC atoms and $g_{\text{BB}} = 2\pi a_{\text{BB}}/m$ describes their

mutual interaction with a_{BB} the s-wave scattering length ($\hbar = 1$). The Bogoliubov dispersion relation reads $\omega_{\mathbf{k}} = ck\sqrt{1 + k^2\xi^2/2}$ with $c = \sqrt{g_{\text{BB}}n_0/m}$ denoting the speed of sound and $k = |\mathbf{k}|$. In order to formally decouple the impurity we transform to a co-moving frame [44] using $\hat{U} = \exp\{-i\hat{r} \cdot \hat{\mathbf{P}}_{\text{ph}}\}$, where $\hat{\mathbf{P}}_{\text{ph}} = \sum_{\mathbf{k}} \mathbf{k} \hat{a}_{\mathbf{k}}^\dagger \hat{a}_{\mathbf{k}}$ is the total phonon momentum. Using $\hat{U}^\dagger \hat{p} \hat{U} = \hat{p} - \sum_{\mathbf{k}} \mathbf{k} \hat{a}_{\mathbf{k}}^\dagger \hat{a}_{\mathbf{k}}$ and $\hat{U}^\dagger \hat{a}_{\mathbf{k}} \hat{U} = \hat{a}_{\mathbf{k}} e^{-i\mathbf{k} \cdot \hat{r}}$, the Hamiltonian reads [36]

$$\begin{aligned} H^{\text{LLP}}(\hat{\mathbf{p}}) &= \frac{1}{2M} \left(\hat{\mathbf{p}} - \sum_{\mathbf{k}} \mathbf{k} \hat{a}_{\mathbf{k}}^\dagger \hat{a}_{\mathbf{k}} \right)^2 + \sum_{\mathbf{k}} \omega_{\mathbf{k}} \hat{a}_{\mathbf{k}}^\dagger \hat{a}_{\mathbf{k}} + g_{\text{IB}} n_0 \\ &+ \frac{g_{\text{IB}}}{L^{d/2}} \sum_{\mathbf{k}} n_0^{1/2} W_{\mathbf{k}} (\hat{a}_{\mathbf{k}} + \hat{a}_{-\mathbf{k}}^\dagger) \\ &+ \frac{g_{\text{IB}}}{2L^d} \sum_{\mathbf{k}, \mathbf{k}'} \left[V_{\mathbf{k}, \mathbf{k}'}^+ \hat{a}_{\mathbf{k}}^\dagger \hat{a}_{\mathbf{k}'} + \frac{1}{2} V_{\mathbf{k}, \mathbf{k}'}^- (\hat{a}_{\mathbf{k}}^\dagger \hat{a}_{-\mathbf{k}'}^\dagger + \hat{a}_{-\mathbf{k}} \hat{a}_{\mathbf{k}'}') \right], \end{aligned} \quad (1)$$

where $V_{\mathbf{k}, \mathbf{k}'}^\pm = (W_{\mathbf{k}} W_{\mathbf{k}'} \pm W_{\mathbf{k}}^{-1} W_{\mathbf{k}'}^{-1})$. $\hat{\mathbf{p}}$ now represents the total momentum of the system which is a constant of motion [45]. In the polaron frame the phonon dynamics attains a nonlinear term $\sim \hat{\mathbf{P}}_{\text{ph}}^2$, which describes impurity-mediated phonon-phonon interactions that vanish in the limit $M \rightarrow \infty$. The impurity-BEC interaction strength $g_{\text{IB}} = 2\pi a_{\text{IB}}/m_{\text{red}}$ is expressed in terms of the s-wave scattering length a_{IB} and reduced mass $m_{\text{red}} = mM/(m + M)$, and $W_{\mathbf{k}} = [k^2\xi^2/(2 + k^2\xi^2)]^{1/4}$. Crucially note that, due to thermal depletion, the condensate fraction $n_0 = n_0(T)$ is temperature dependent. For weak Bose-Bose interactions we have $n_0(T)/n = 1 - (T/T_c)^{3/2}$ at fixed total particle density n .

Polaron properties are encoded in the impurity Green's function $S(t) = \text{Tr}\{e^{iH_0 t} e^{-iH t} \rho\}$, where the density matrix ρ determines the initial state of the system, and H_0 and H are the Hamiltonian in absence and presence of the impurity bath interaction. $S(t)$, also called ‘‘dynamical overlap,’’ describes the dephasing dynamics of the system following a sudden quench of g_{IB} at time $t = 0$. It can be measured using Ramsey spectroscopy as previously demonstrated in fermionic environments [12,13,33,34]. Fourier transformation of $S(t)$ in turn yields the (injection) absorption spectrum $A(\omega) = 2\text{Re} \int_0^\infty d\tau e^{i\omega\tau} S(\tau)$ in linear response, when the impurity is driven from a noninteracting state to a state with finite g_{IB} [13,26,28,34].

In contrast to previous studies of this problem [36,38,42,43,46–59], we here consider finite temperature. This is accounted for by an initial density matrix $\rho = \rho_T^{\text{ph}} \otimes |\mathbf{p}\rangle\langle\mathbf{p}|$, where the phonon bath is in thermal equilibrium, $\rho_T^{\text{ph}} = e^{-\beta \sum_{\mathbf{k}} \omega_{\mathbf{k}} \hat{a}_{\mathbf{k}}^\dagger \hat{a}_{\mathbf{k}}} / Z$ ($Z = \text{Tr}[e^{-\beta H_0}]$), for an impurity initially in a momentum eigenstate $|\mathbf{p}\rangle$. In order to unambiguously identify the role of bath temperature and to allow direct comparison with previous studies [41],

we focus in the following on $\mathbf{p} = 0$. An important simplification of the $T = 0$ limit is that the initial state is invariant under the Lee-Low-Pines transformation, which is no longer the case at finite T . Here the total momentum $\hat{\mathbf{P}}_{\text{ph}}$ appearing in H^{LLP} has rms fluctuations that are extensive in the system size. We will show in the following that a proper generalization of the dynamical variational approach of Ref. [43] solves this problem. To this end we first introduce a projector $\hat{\Pi}_{\mathbf{Q}}$ on eigenstates of $\hat{\mathbf{P}}_{\text{ph}}$ with eigenvalue \mathbf{Q} . Then one finds $U^\dagger \rho U = \int d^3 Q \hat{\Pi}_{\mathbf{Q}} \rho_T^{\text{ph}} \otimes |\mathbf{p} + \mathbf{Q}\rangle\langle \mathbf{p} + \mathbf{Q}|$. We represent the thermal state of phonons as a Gaussian average over coherent states $|\xi_k\rangle$ [60]: $\rho_T^{\text{ph}} = \prod_k \int d^2 \xi_k [e^{-|\xi_k|^2/\bar{n}_k/\pi\bar{n}_k}] |\xi_k\rangle\langle \xi_k|$. Here $\bar{n}_k = 1/(e^{\beta\omega_k} - 1)$ is the average phonon number in mode k . Thus we find

$$S(t) = \int d^3 Q \overline{\langle \psi_0(t) | \hat{\Pi}_{\mathbf{Q}} | \psi(t) \rangle}. \quad (2)$$

Here $|\psi(t)\rangle = e^{-iH^{\text{LLP}}(\mathbf{Q})t} |\xi_k\rangle$ and $|\psi_0(t)\rangle = e^{-iH_0^{\text{LLP}}(\mathbf{Q})t} |\xi_k\rangle$ describe the time evolution of the initial states $|\xi_k\rangle$ under $H^{\text{LLP}}(\mathbf{Q})$ and $H_0^{\text{LLP}}(\mathbf{Q})$ (Eq. (1) for $g_{\text{IB}} = 0$), respectively, where the impurity-momentum operator $\hat{\mathbf{p}}$ is replaced by the c number \mathbf{Q} . The overbar denotes the average over the ξ_k 's and we have used that H_0^{LLP} commutes with the projector $\hat{\Pi}_{\mathbf{Q}}$.

Dynamical variational ansatz.—We calculate $S(t)$ using wave functions $|\psi(t)\rangle$ and $|\psi_0(t)\rangle$ in a variational submanifold of Hilbert space constructed by time-dependent multimode coherent states $|\beta(t)\rangle = \prod_k e^{\beta_k \hat{a}_k^\dagger - \text{H.c.}} |0\rangle = \prod_k |\beta_k(t)\rangle$ including a time-dependent phase $|\psi(t)\rangle = e^{-i\phi(t)} |\beta(t)\rangle$. With $|\psi_0(t)\rangle = e^{-i\phi_0(t)} |\beta^0(t)\rangle$, and defining $\Delta\phi \equiv \phi - \phi_0$ one finds $S(t) = \int d^3 Q e^{-i\Delta\phi(t)} \overline{\langle \beta^0(t) | \hat{\Pi}_{\mathbf{Q}} | \beta(t) \rangle}$. The minimization of the Lagrangian $\mathcal{L} = \langle \psi(t) | i\partial_t - H^{\text{LLP}} | \psi(t) \rangle$, and similarly \mathcal{L}_0 , gives the Euler-Lagrange equations $d/dt(\partial\mathcal{L}/\partial\dot{\beta}_k) - \partial\mathcal{L}/\partial\beta_k = 0$,

$$\begin{aligned} i \frac{d}{dt} \beta_k(t) &= \left(\omega_k + \frac{k^2}{2M} - \frac{k}{M} \cdot (\mathbf{Q} - \mathbf{P}_{\text{ph}}) \right) \beta_k(t) \\ &+ \frac{g_{\text{IB}} \sqrt{n_0}}{L^{d/2}} W_k + \frac{g_{\text{IB}}}{L^d} \sum_q (W_k W_q \text{Re}[\beta_q(t)] \\ &+ i W_k^{-1} W_q^{-1} \text{Im}[\beta_q(t)]), \end{aligned} \quad (3)$$

and similarly for $\beta_k^0(t)$ (where $g_{\text{IB}} = 0$), with (random) initial values $\beta_k(0) = \beta_k^0(0) = \xi_k$. The total phonon momentum in state $|\psi(t)\rangle$ is given by $\mathbf{P}_{\text{ph}} = \sum_k \mathbf{k} |\beta_k(t)|^2$. The time-dependent Schrödinger equation implies $\mathcal{L} = \mathcal{L}_0 = \text{const}$, and thus,

$$i \frac{d\Delta\phi}{dt} = g_{\text{IB}} \left(n_0 + \sqrt{\frac{n_0}{L^d}} \sum_k W_k \beta_k'(t) \right) - \frac{(\mathbf{P}_{\text{ph}} - \mathbf{P}_{\text{ph}}^0)^2}{2M}, \quad (4)$$

with $\beta_k' = \text{Re}[\dot{\beta}_k]$. Note that different from $T = 0$, also the phonon momentum \mathbf{P}_{ph}^0 without interactions enters.

Infinitely heavy impurity.—We first discuss the limit of an infinitely heavy impurity, $M \rightarrow \infty$. In this case $H_0^{\text{LLP}}(\mathbf{Q})$ and $H^{\text{LLP}}(\mathbf{Q})$ become independent of \mathbf{Q} and Eq. (2) becomes

$$S(t) = \overline{e^{-i\Delta\phi(t)} \langle \beta^0(t) | \beta(t) \rangle}. \quad (5)$$

Moreover, the equations of motion (EOM) for $\beta_k(t)$, $\beta_k^0(t)$, and $\Delta\phi(t)$ become linear. This allows one to express the overlap $\langle \beta^0(t) | \beta(t) \rangle$ as a matrix-Gaussian function in terms of the random initial variables ξ_k , and the thermal average can be carried out analytically (see Ref. [61]). For $g_{\text{BB}} = 0$ our coherent state approach becomes exact and we have verified that our results match those from a functional determinant approach [5]. Equation (5) allows one to determine the temperature dependence of $S(t)$ and from its Fourier transform the absorption spectrum as shown in Fig. 2 for a fixed impurity-bath interaction strength. One notices a substantial broadening with increasing temperature accompanied with a small shift of the peak position.

Finite impurity mass.—For a finite impurity mass the variational states are \mathbf{Q} dependent and the corresponding integration in Eq. (2) cannot be carried out up front. Furthermore the EOM Eq. (3) become nonlinear due to the presence of the total phonon momentum \mathbf{P}_{ph} . For $T = 0$, \mathbf{P}_{ph} is proportional to the conserved polaron momentum and thus vanishes in the case of an impurity initially at rest. This does not hold, however, at finite temperatures where \mathbf{P}_{ph} also contains the random initial amplitudes ξ_k . For these reasons the case of a finite impurity mass is substantially more involved compared to zero temperature even within the coherent-state variational approach and one has to resort to approximations.

First, the projector on total-momentum eigenstates can be written as $\hat{\Pi}_{\mathbf{Q}} = [1/(2\pi)^3] \int d^3 z e^{iz \cdot (\hat{\mathbf{P}}_{\text{ph}} - \mathbf{Q})}$ where the action of the operator $e^{iz \cdot \hat{\mathbf{P}}_{\text{ph}}} = \prod_k e^{iz \cdot \mathbf{k} \hat{a}_k^\dagger \hat{a}_k}$ can be absorbed in a phase shift of the coherent amplitudes $\beta_k^0(t) \rightarrow \beta_k^0(t) e^{-iz \cdot \mathbf{k}}$. Thus evaluating $S(t)$ for a finite impurity mass is formally analogous to the infinite-mass case, however, demanding two additional integrations $\int d^3 z$ and $\int d^3 Q$, which presents a numerical challenge. To address this issue, we here replace the phonon-momentum operator in $\hat{\Pi}_{\mathbf{Q}}$ by its expectation value with respect to the variational wave function, followed by an average over the random thermal amplitudes, i.e., $e^{iz \cdot \hat{\mathbf{P}}_{\text{ph}}} \rightarrow e^{iz \cdot \overline{\mathbf{P}}_{\text{ph}}}$. For an impurity initially at rest one has $\overline{\mathbf{P}}_{\text{ph}} = 0$ and $\hat{\Pi}_{\mathbf{Q}}$ becomes

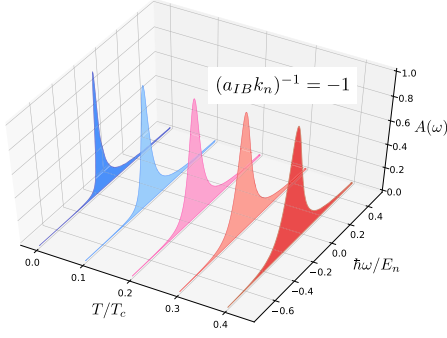


FIG. 2. Absorption spectrum for attractive polaron for infinitely heavy impurity $M = \infty$ at different temperatures, and Bose-Bose interaction strength $k_n a_{\text{BB}} = 0.01$. While increasing T/T_c leads to a shift of the line center and a substantial broadening of the quasiparticle peak, no new quasiparticle peaks appear.

the unity operator $\hat{\Pi}_Q \rightarrow \delta^{(3)}(\mathbf{Q} - \overline{\mathbf{P}}_{\text{ph}}) = \delta^{(3)}(\mathbf{Q})$. The \mathbf{Q} integration is then trivial and $S(t)$ obeys again Eq. (5), where $\beta_k(t)$, $\beta_k^0(t)$, and $\Delta\phi(t)$ now, however, follow Eqs. (3) and (4) for a finite-mass impurity.

Accordingly, the EOM of $\beta_k(t)$ and $\beta_k^0(t)$, which are given by Eq. (3) with $\mathbf{Q} = 0$, are still nonlinear. As outlined in Ref. [61], the nonlinear terms in Eqs. (3) and (4) can be approximated by a mean-field ansatz, where the quantities $\mathbf{P}_{\text{ph}}\beta_k(t)$ and $(\mathbf{P}_{\text{ph}} - \mathbf{P}_{\text{ph}}^0)^2$ are effectively replaced by $k\bar{n}_k\beta_k(t)$, and $2\sum_k k^2\bar{n}_k(|\beta_k(t)|^2 - |\xi_k|^2)$, respectively. To this end we note that at $t = 0$ the $\beta_k(t)$ are Gaussian random variables given by ξ_k and we can assume that they remain Gaussian for all times. This finally renders the EOM for $\beta_k(t)$ in a linear form that is amenable to an analytical solution. Note that the equation for the total phase remains nonlinear but can be readily integrated. As a result the dynamical overlap can be expressed as matrix-Gaussian functions in terms of ξ_k and the thermal averaging can be carried out analytically. Most importantly the finite-temperature dynamical overlap can then be written as a product of the $T = 0$ result $S_0(t)$ and a finite-temperature factor $f_T(t)$,

$$S(t) = f_T(t)S_0(t), \quad (6)$$

whose explicit analytic form is given in the Supplemental Material [61].

The dynamical overlap $S(t)$ calculated in this way is shown in Fig. 3(a) as a function of time. Results are shown for the attractive polaron for increasing temperatures in units of the critical temperature $T_c = (2\pi/m)[n/\zeta(3/2)]^{2/3}$ of a noninteracting gas in a box. While for zero temperature $S(t)$ reproduces exactly the result from Ref. [43] and approaches a finite value at large times given by the zero-temperature quasiparticle weight, it decays exponentially for $T > 0$ with an asymptotic behavior $|S(t)| \sim Z(T)e^{-\gamma(T)t}$. The decay rates $\gamma(T)$ and thermal weights $Z(T)$ obtained from fits of the asymptotic tails are plotted in

Figs. 3(b) and 3(c) as a function of T/T_c for different impurity-Boson interaction strengths (for more details on the analysis of emerging, subleading quasiparticle branches, see Ref. [61]). One recognizes an asymptotic power-law scaling of both quantities as a function of T/T_c . While this is reminiscent to the fermionic case [5], where the exponents are given by the scattering phase shift at the Fermi momentum, it remains an open question to find analytical expressions for the exponents in the case of Bose polarons where no such a special finite momentum exists and scattering should predominantly take place at small momenta, or a momentum scale $\sim\sqrt{k_B T}$ determined by the thermal de Broglie wavelength (at sufficiently large T). Remarkably, we find that close to unitary interactions the broadening of the quasiparticle peak, determined by $\gamma(T)$, shows a crossover to a linear temperature dependence, which may be attributed to quantum critical behavior of impurities in a Bose gas [39].

From the Fourier transform of $S(t)$, such as shown in Fig. 3(a), we have calculated the absorption spectrum for parameters of the experiment of Jørgensen *et al.* [38] and [42]. The result, shown in Fig. 1, is in good agreement with the experiment. The peak positions extracted from the numerical simulations (red points) on the repulsive side coincide with the experimental values (green points) determined by Gaussian fits. In order to take into account the inhomogeneous density distribution in the experiment and the finite resolution of the spectrometer, we have made a trap average, weighted by the BEC density, assuming a Thomas-Fermi distribution. By convolution, we included a Gaussian broadening using the experimental parameters from Ref. [38]. On the attractive side the experimental values for the lowest polaron branch, extracted from the onset of the measured absorption spectrum (purple points), agree with the onset of the absorption spectrum obtained from our numerical simulations.

Summary.—We discussed the physics of a single, mobile quantum impurity interacting with a BEC of atoms at finite temperature. Extending the dynamical variational approach of Ref. [43] to the case of an initial thermal state of Bogoliubov phonons, we showed how thermal effects enter the Hamiltonian in the Lee-Low-Pines frame that is used to decouple the impurity from the phonon dynamics. To describe polaron formation we calculated the real-time polaron Green's function $S(t)$ and from it the absorption spectrum $A(\omega)$ for a transition of the impurity from a state noninteracting to a state interacting with the environment. Strong impurity-BEC interactions are accounted for by the inclusion of two-phonon terms in the Hamiltonian [36]. Within the proposed variational approach one restricts the dynamics to a submanifold of coherent-state wave functions that are thermally averaged with Gaussian, random initial amplitudes, with weights determined by the temperature. While in the limit of an infinitely heavy impurity, the EOMs become linear and the thermal average can be

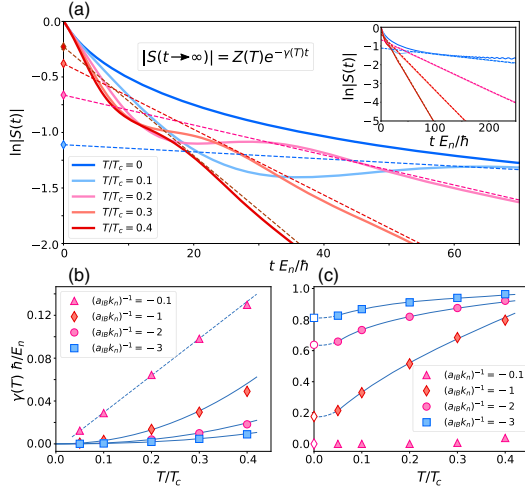


FIG. 3. (a) Impurity Green's function $S(t)$ of an attractive polaron with $k_n a_{IB} = -1$ for increasing (from top to bottom) temperatures for $m = M$ and $k_n a_{BB} = 0.01$. While at $T = 0$ the overlap $|S(t)|$ approaches a finite value, it turns into an asymptotic exponential decay for $T > 0$. Extrapolating the exponential to $t = 0$ defines a finite-temperature weight $Z(T)$. (b) Decay rate as function of T/T_c obtained from fits to exponential tails. Close to unitary interactions a linear temperature dependence is found (dashed), linked to quantum critical behavior in Ref. [39]. (c) Thermal weights $Z(T)$, where empty symbols show values for $T = 0$. As guide to the eye for interaction strength $(k_n a_{IB})^{-1} = (-1; -2; -3)$ asymptotic power-law fits for $\gamma(T) \sim (T/T_c)^\nu$ and $Z(T) \sim (T/T_c)^\mu$ are shown with exponents $\nu = (2.10; 2.28; 2.35)$ and $\mu = (0.65; 0.16; 0.07)$.

performed analytically, for a finite impurity mass a mean-field approximation is required to allow for an analytical thermal average. We calculated the temperature dependence of $S(t)$ for different interaction strengths, and found an asymptotic exponential decay $S(t) \sim Z(T)e^{-\gamma(T)t}$. The extracted decay rates $\gamma(T)$ and thermal weights $Z(T)$ show a power-law dependence on T/T_c . Close to unitarity, $1/k_n a = 0$, the inverse polaron quasiparticle lifetime shows a linear dependence on temperature that is indicative of non-Fermi liquid behavior in the vicinity of the underlying quantum critical point [39]. The comparison of the theoretical absorption spectra with a recent experiment [38,42] shows that the inclusion of finite temperature corrections leads to excellent agreement between theory and experiment on the repulsive side that was lacking in previous comparisons with $T = 0$ calculations. Our results are also in excellent agreement with the measured lowest polaron branch as well as the widths of the absorption spectra. In contrast to recent T -matrix calculations [41] we do not find a splitting or separate temperature-induced quasiparticle peaks of substantial spectral weight.

The authors like to thank N. Jørgensen and J. Arlt for providing the experimental data from Ref. [38]. We also thank G. Bruun, E. Demler, P. Massignan, Y. Shchadilova,

and M. Zwierlein for useful comments and discussions. The work of D. D. and M. F. has been supported by the Deutsche Forschungsgemeinschaft (DFG, German Research Foundation) within the SFB-TR 185–277625399. R. S. is supported by the Deutsche Forschungsgemeinschaft (DFG, German Research Foundation) under Germany's Excellence Strategy—EXC-2111–390814868.

- [1] L. Landau and S. Pekar, *J. Exp. Theor. Phys.* **423**, 71 (1948).
- [2] L. D. Landau, *Phys. Z. Sowjetunion* **3**, 664 (1933).
- [3] C. Chin, R. Grimm, P. Julienne, and E. Tiesinga, *Rev. Mod. Phys.* **82**, 1225 (2010).
- [4] F. Camargo, R. Schmidt, J. D. Whalen, R. Ding, G. Woehl, S. Yoshida, J. Burgdörfer, F. B. Dunning, H. R. Sadeghpour, E. Demler, and T. C. Killian, *Phys. Rev. Lett.* **120**, 083401 (2018).
- [5] R. Schmidt, H. R. Sadeghpour, and E. Demler, *Phys. Rev. Lett.* **116**, 105302 (2016).
- [6] J. Sous, H. Sadeghpour, T. Killian, E. Demler, and R. Schmidt, *Phys. Rev. Research* **2**, 023021 (2020).
- [7] A. Schirotzek, C.-H. Wu, A. Sommer, and M. W. Zwierlein, *Phys. Rev. Lett.* **102**, 230402 (2009).
- [8] Y. Zhang, W. Ong, I. Arakelyan, and J. E. Thomas, *Phys. Rev. Lett.* **108**, 235302 (2012).
- [9] C. Kohstall, M. Zaccanti, M. Jag, A. Trenkwalder, P. Massignan, G. M. Bruun, F. Schreck, and R. Grimm, *Nature (London)* **485**, 615 (2012).
- [10] M. Koschorreck, D. Pertot, E. Vogt, B. Fröhlich, M. Feld, and M. Köhl, *Nature (London)* **485**, 619 (2012).
- [11] F. Scazza, G. Valtolina, P. Massignan, A. Recati, A. Amico, A. Burchianti, C. Fort, M. Inguscio, M. Zaccanti, and G. Roati, *Phys. Rev. Lett.* **118**, 083602 (2017).
- [12] M. Cetina, M. Jag, R. S. Lous, J. T. M. Walraven, R. Grimm, R. S. Christensen, and G. M. Bruun, *Phys. Rev. Lett.* **115**, 135302 (2015).
- [13] M. Cetina, M. Jag, R. S. Lous, I. Fritsche, J. T. M. Walraven, R. Grimm, J. Levinsen, M. M. Parish, R. Schmidt, M. Knap, and E. Demler, *Science* **354**, 96 (2016).
- [14] M. M. Parish and J. Levinsen, *Phys. Rev. B* **94**, 184303 (2016).
- [15] F. Chevy, *Phys. Rev. A* **74**, 063628 (2006).
- [16] C. Lobo, A. Recati, S. Giorgini, and S. Stringari, *Phys. Rev. Lett.* **97**, 200403 (2006).
- [17] R. Combescot, A. Recati, C. Lobo, and F. Chevy, *Phys. Rev. Lett.* **98**, 180402 (2007).
- [18] S. Pilati and S. Giorgini, *Phys. Rev. Lett.* **100**, 030401 (2008).
- [19] M. Punk, P. T. Dumitrescu, and W. Zwerger, *Phys. Rev. A* **80**, 053605 (2009).
- [20] N. Prokof'ev and B. Svistunov, *Phys. Rev. B* **77**, 020408(R) (2008).
- [21] N. V. Prokof'ev and B. V. Svistunov, *Phys. Rev. B* **77**, 125101 (2008).
- [22] C. Mora and F. Chevy, *Phys. Rev. A* **80**, 033607 (2009).
- [23] P. Kroiss and L. Pollet, *Phys. Rev. B* **90**, 104510 (2014).
- [24] P. Kroiss and L. Pollet, *Phys. Rev. B* **91**, 144507 (2015).

- [25] O. Goulko, A. S. Mishchenko, N. Prokof'ev, and B. Svistunov, *Phys. Rev. A* **94**, 051605(R) (2016).
- [26] R. Schmidt and T. Enss, *Phys. Rev. A* **83**, 063620 (2011).
- [27] X. Cui and H. Zhai, *Phys. Rev. A* **81**, 041602(R) (2010).
- [28] P. Massignan and G. M. Bruun, *Eur. Phys. J. D* **65**, 83 (2011).
- [29] P. Massignan, M. Zaccanti, and G. M. Bruun, *Rep. Prog. Phys.* **77**, 034401 (2014).
- [30] R. Schmidt, T. Enss, V. Pietilä, and E. Demler, *Phys. Rev. A* **85**, 021602(R) (2012).
- [31] V. Ngampruetikorn, J. Levinsen, and M. M. Parish, *Europhys. Lett.* **98**, 30005 (2012).
- [32] J. Goold, T. Fogarty, N. Lo Gullo, M. Paternostro, and T. Busch, *Phys. Rev. A* **84**, 063632 (2011).
- [33] M. Knap, A. Shashi, Y. Nishida, A. Imambekov, D. A. Abanin, and E. Demler, *Phys. Rev. X* **2**, 041020 (2012).
- [34] R. Schmidt, M. Knap, D. A. Ivanov, J.-S. You, M. Cetina, and E. Demler, *Rep. Prog. Phys.* **81**, 024401 (2018).
- [35] S. I. Mistakidis, G. C. Katsimiga, G. M. Koutentakis, and P. Schmelcher, *New J. Phys.* **21**, 043032 (2019).
- [36] S. P. Rath and R. Schmidt, *Phys. Rev. A* **88**, 053632 (2013).
- [37] M. G. Hu, M. J. Van De Graaff, D. Kedar, J. P. Corson, E. A. Cornell, and D. S. Jin, *Phys. Rev. Lett.* **117**, 055301 (2016).
- [38] N. B. Jørgensen, L. Wacker, K. T. Skalmstang, M. M. Parish, J. Levinsen, R. S. Christensen, G. M. Bruun, and J. J. Arlt, *Phys. Rev. Lett.* **117**, 055302 (2016).
- [39] Z. Z. Yan, Y. Ni, C. Robens, and M. W. Zwierlein, *Science* **368**, 190 (2020).
- [40] J. Levinsen, M. M. Parish, R. S. Christensen, J. J. Arlt, and G. M. Bruun, *Phys. Rev. A* **96**, 063622 (2017).
- [41] N.-E. Guenther, P. Massignan, M. Lewenstein, and G. M. Bruun, *Phys. Rev. Lett.* **120**, 050405 (2018).
- [42] L. A. Peña Ardila, N. B. Jørgensen, T. Pohl, S. Giorgini, G. M. Bruun, and J. J. Arlt, *Phys. Rev. A* **99**, 063607 (2019).
- [43] Y. E. Shchadilova, R. Schmidt, F. Grusdt, and E. Demler, *Phys. Rev. Lett.* **117**, 113002 (2016).
- [44] T. Lee, F. Low, and D. Pines, *Phys. Rev.* **341**, 297 (1953).
- [45] M. Girardeau, *Phys. Fluids* **4**, 279 (1961).
- [46] S. I. Mistakidis, G. C. Katsimiga, G. M. Koutentakis, T. Busch, and P. Schmelcher, *Phys. Rev. Lett.* **122**, 183001 (2019).
- [47] A. Camacho-Guardian, L. A. Peña Ardila, T. Pohl, and G. M. Bruun, *Phys. Rev. Lett.* **121**, 013401 (2018).
- [48] K. K. Nielsen, L. A. P. Ardila, G. M. Bruun, and T. Pohl, *New J. Phys.* **21**, 043014 (2019).
- [49] J. Levinsen, M. M. Parish, and G. M. Bruun, *Phys. Rev. Lett.* **115**, 125302 (2015).
- [50] M. Sun, H. Zhai, and X. Cui, *Phys. Rev. Lett.* **119**, 013401 (2017).
- [51] L. A. Pena Ardila and S. Giorgini, *Phys. Rev. A* **92**, 033612 (2015).
- [52] M. Will, T. Lausch, and M. Fleischhauer, *Phys. Rev. A* **99**, 062707 (2019).
- [53] F. Grusdt, R. Schmidt, Y. E. Shchadilova, and E. Demler, *Phys. Rev. A* **96**, 013607 (2017).
- [54] F. Grusdt, K. Seetharam, Y. Shchadilova, and E. Demler, *Phys. Rev. A* **97**, 033612 (2018).
- [55] Y. Ashida, R. Schmidt, L. Tarruell, and E. Demler, *Phys. Rev. B* **97**, 060302(R) (2018).
- [56] M. Leshchko and R. Schmidt, [arXiv:1703.06753](https://arxiv.org/abs/1703.06753).
- [57] B. Midya, M. Tomza, R. Schmidt, and M. Leshchko, *Phys. Rev. A* **94**, 041601(R) (2016).
- [58] M. Drescher, M. Salmhofer, and T. Enss, *Phys. Rev. A* **99**, 023601 (2019).
- [59] A. G. Volosniev, H.-W. Hammer, and N. T. Zinner, *Phys. Rev. A* **92**, 023623 (2015).
- [60] M. O. Scully and M. S. Zubairy, *Quantum Optics* (Cambridge University Press, Cambridge, 1997).
- [61] See Supplemental Material at <http://link.aps.org/supplemental/10.1103/PhysRevLett.124.223401> for further details about the calculations. Here, we explain in more depth how to solve the equations of motion for the dynamical variables and how to perform the thermal averaging. Also, details are given about the trap averaging, as well as about the spectral analysis of the Ramsey signal.